PLASMA LENSES

J.J.Su, T.Katsouleas and J.M.Dawson
University of California at Los Angeles
Department of Physics
Los Angeles, CA 90024

Abstract The focusing of particles by a thin plasma lens is analyzed with physical, linearized fluid and PIC computational models. For parameters similar to the next-generation linear colliders, the plasma lens strength can exceed 100 MGauss/cm, and the luminosity can be enhanced by an order of magnitude by passing each beam through an appropriate plasma slab. Both overdense and underdense plasma lenses are described (plasma density n_0 greater or less than beam density n_b). The former case applies equally well to e^+ and e^- beams, while the latter has distinct advantages for e^- beams (including smaller aberrations and background). The effects of spherical and longitudinal aberrations and beam-beam disruption are disscussed.

Introduction

One of the challenges for future e^+e^- high energy colliders is to increase the luminosity as the square of the center of mass energy in order to keep the event rate constant. For fixed repetition rate and number of particles this means reducing the spot size of the beams at the interaction point. Recently, plasma techniques capable of exteremely strong focusing gradients (order 100 MG/cm compared to 5kG/cm for typical quadrupole magnets) have been proposed to accomplish such size reduction [1-2].

At least three distinct particle focusing schemes in plasmas have been referred to as plasma lenses. Theee are (1)focusing of particles by the radial fields of a large-amplitude plasma wave moving with the beam [3,4], (2)focusing by the aximuthal magnetic field of a z-pinch wave carrying a large axial current [5,6], and (3)self-focusing due to shielding of a particle beam's space charge by a quiescent plasma[1,2,7]. It is this latter plasma lens concept that will be examined here.

Previous work on self-pinch plasma lens has been mainly devoted to analytic models in the overdense plasma regime. Here we consider both overdense and underdense plasma lenses. Simple physical models and analytic predictions are compared to 2-D self-consistent particle-in-cell simulations. The results are discussed with examples given for presently available beam parameters and the parameter proposed for future colliders[8].

Overdense Plasma Lenses ($n_b \ll n_0$)

The overdense plasma lens operates in the regime where the beam density n_b represents a small perturbation to the plasma density n_0. In this case the plasma dynamics can be described by linear theory for both electrons and positrons.

Consider a relativistic electron beam traveling through vacuum. In this case the repulsive Coulomb force cancels the attractive Lorentz force; thus the beam continues with essentially constant radius. However, if this beam now enters a plasma, the plasma electrons respond to the excess charge by shiffting away from the beam particles. The remaining plasma ions neutralize the space charge force within the beam. While the palsma is effective at shielding the beam's space charge, the beam experiences almost the full effect of its self-generated azimuthal magnetic field. From Ampere's law this is $B_\theta = 2\pi n_b e r$ for a uniform beam density n_b. This gives a radial Lorentz force

$$F_r \sim 2\pi n_b e^2 r \tag{.1}$$

$$\frac{F_r}{r} \simeq 2\pi n_b e^2 \simeq 3\times 10^{-9} n_b \, gauss/cm \tag{.2}$$

for n_b in cm^{-3}. For example,a beam has density $n_b \sim 10^{17} cm^{-3}$ and $F_r/r \sim 300 megagauss/cm$. This exceeds by four order of magnitude the equivalent focusing strength of conventional quadrupole magnets. Neglecting aberrations, the beam radius σ at I.P. is inversely proportional to the focusing strength of the final lens (for fixed lens thickness and beam emittance), and the luminosity $\mathcal{L}$ is proportional to σ^{-2}. Thus the luminosity enhancement from a plasma lens may be considerable.

A formal wakefield analysis of the plasma lens using a cold plasma model has been given previously in Refs. 1 and 2. Here we summarize the results and apply them to determining the aberrations of the lens.

The transverse wakefield is defined as the transverse Lorentz force on a unit charge moving with velocity $\beta = v/c \simeq 1$ in the logitudinal direction:

$$W_\perp(r,\zeta) = (\vec{E} + \vec{\beta}\times\vec{B})_r \simeq E_r - B_\theta \tag{.3}$$

where the plasma wake is assumed to be a function only of r and $\zeta = z - ct$. The wakefield excited by a relativistic beam of arbitrary density in the form $n_b = \rho_\parallel(\zeta)\rho_\perp(r)$ is[1]

$$W_\perp = Z(\zeta)\frac{\partial}{\partial r}R(r) \tag{.4}$$

where

$$Z(\zeta) = -\frac{4\pi e\rho_b}{k_p^2}\int_\infty^\zeta d\zeta' \rho_\parallel(\zeta')\cos k_p(\zeta-\zeta')$$

$$R(r) = \int_0^\infty r' dr' \rho_\perp(r') I_0(k_p r_<) K_0(k_p r_>)$$

where $k_p = 2\pi\omega_p/c$.

Analytic and numerical solutions of these integrals have been obtain previously by several authors[1-2,9] for various density profiles. For example, a Gaussian $\rho_\perp = \rho_0 \exp(-r^2/2\sigma^2)$ profile is illustrated in Fig. 1 for $\sigma = 2c/\omega_p$. Figure 1.b illustrates the need to keep the spot size small compare to the plasma skin depth in order to minimize the aberrations.

We now return to the z-dependence of the radial wakefield in Eq(5). As we see from Eq.(5) the solutions to $W_\perp$ in general oscillate in z with period k_p^{-1}. When the plasma electrons are displaced by the particle beam they tend to overshoot and oscillate. A simple solution is to allow the beam density to increase slowly at the head compared to c/ω_p. In this way the plasma electrons respond adiabatically without oscillating appreciably.

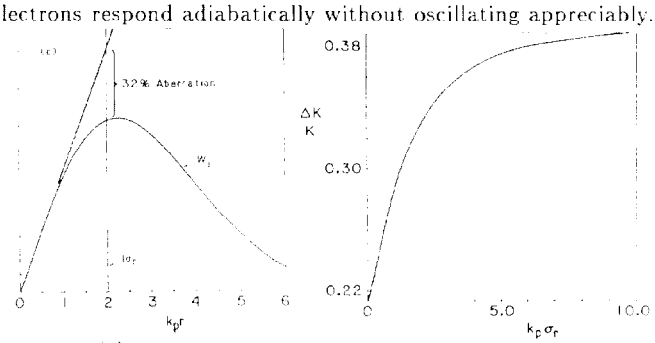

Figure .1: (a). The focusing force $w_\perp$ vs. r for a Gaussian profile , $\sigma = 2c/\omega_p$. (b) Spherical aberration ($= 1 - \frac{W_\perp}{r}(\sigma_r)/\frac{W_\perp}{r}(0)$), where σ_r is the r.m.s radius of the beam, vs. beam radius.

CH2669-0/89/0000-0894$01.00©1989 IEEE

The longer in the scale length of beam density compared to the plasma skin depth the smaller are the oscillations in the focusing force. Thus for beams ramped slowly compare to c/ω_p the focusing force follows the beam shapes in the logitudinal direction. The variation in focusing strength gives rise to a logitudinal aberration of the plasma lens that will be discussed in a later section.

Two limitations on the final spot size of a particle beam result from the emittance of the beam and the aberrations of the lens. Here we use beam optics and the wakefields results to obtain scaling laws for the final spot size.

Form beam optics[10,11], the minimum waist of a freely propagating beam is

$$a^{*2} = \frac{a_0^2}{1+\beta_0^2/f^2} \qquad (.5)$$

where a_0 is the beam radius at the lens, f is the lens' focal length and β_0 is the beta function at the lens entrance.

A particle at r.m.s. radius a_0 entering the lens is given a radial deflection θ proportional to the focusing strength (K) at radius a_0. If the lens has aberrations ΔK, then the particle will recive an error in radial kick by an amount $\Delta\Theta = \Theta(\Delta K/K)$, where $\Theta \simeq a_0/f$, so that the final spot size is $f\Delta\Theta$ or

$$a^* \geq a_0 \frac{\Delta K}{K} \qquad (.6)$$

Spherical aberrations will also increase the emittance of the beam. This is clearly seen in the numerical phase plots of Fig. 2. The aberration contribution to emittance growth has been approximated by Rosenzwig, *et al.*[10] as the growth of the phase space ellipse. From the figures, we conclude that their analytics results are reasonable for weak focusing; clearly for strong focusing or cooler beams the phase space can not be approximated as an ellipse (Fig. 2b).

Because the focusing force of the overdense plasma lens is determined by the beam's own current profile rather than an externally applied field, the force in general will not be uniform over the length of the beam. For a Gaussian beam, the particles on either end will not focus as tightly as those in the center. This will degrade the luminosity enhancement. The luminosity is given by

$$\mathcal{L} = 2\nu \int\int\int\int_{-\infty}^{\infty} \rho_1 \rho_2 dx\, dy\, dz\, dct \qquad (.7)$$

where $\rho_{1,2}$ are the densities of two beams and ν is the collider's repetition rate. For left and right going beams

$$\rho = \frac{N}{(2\pi)^{3/2}\sigma_r^2\sigma_z} e^{-r^2/2\sigma_r^2 - (z\pm ct)^2/2\sigma_z^2)}$$

where σ_r, the beam radius, is now a function of $z \pm ct$ position due to the logitudinal aberrations. To find σ_r we employ a Twiss parameters anbalysis treating the focusing strength. $K = K_0 \exp(-(z \pm ct)^2/2\sigma_z^2)$ for Gaussian beams and neglect spherical aberrations. Carrying through the algebra we obtain

$$\sigma_{1,2}^2 = \sigma_0^2\{(1 - \frac{z \pm z_0}{f} e^{-(z\mp ct)^2/2\sigma_z^2})^2 + (\frac{z \pm z_0}{\beta_0})^2\} \qquad (.8)$$

for $-z_0 < z < z_0$, where $z_0 = f/(a + f^2/\beta_0^2)$ is the distance from the lenses to the location of minimum beam waist, $f \equiv 1/K_0 l$. Substituting from above for $\sigma_{1,2}$ in Eq. (8), we can integrate Eq. (8) numerically. We obtain

$$\mathcal{L} = \frac{\nu N_1 N_2}{4\pi\sigma^{*2}} \cdot \frac{\mathcal{L}}{\mathcal{L}^*}(\frac{f}{\beta_0}, \frac{\sigma_z}{\beta_0})$$

where $\sigma^{*2} = \sigma_0^2/(1+\beta_0^2/f^2)$ is the minimum spot size of the center of the beam and $\frac{\mathcal{L}}{\mathcal{L}^*}$ is the reduction factor due to the logitudinal dependence of the focusing strength. For $\sigma_z/\beta^* \ll 1$, we observe that $\frac{\mathcal{L}}{\mathcal{L}^*}$ is a function of the single parameter f/β_0. For example, if $f/\beta_0 \simeq 0.1$, we expect $\frac{\mathcal{L}}{\mathcal{L}^*} \approx \frac{\beta_0^2}{\sigma^{*2}} \approx \frac{\beta_0^2}{f^2} \approx 100$ for an aberration free lens. The logitudinal aberration reduction factor for the overdense plasma lens is approximately $\frac{\mathcal{L}}{\mathcal{L}^*} = 0.2$ giving a luminosity enhancement $\frac{\mathcal{L}}{\mathcal{L}_0} \approx 20$ (see Fig. 9b). This factor $\mathcal{L}/\mathcal{L}^*$ *vs* f/β_0 is plotted in Fig. 3 for small σ_z/β_0. For σ_z not small compared to β^* the $\mathcal{L}/\mathcal{L}_0$ is further limited by the spreading of the beams as they pass through each other as described by Erickson[12].

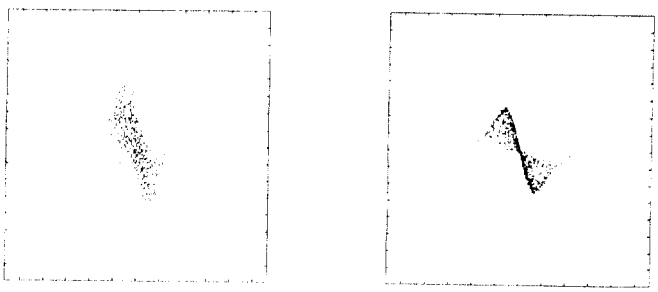

Figure .2: beam phase space at exit of an overdense plasma lens, density $n_p = 5 \times 10^{17} cm^{-3}$ thichness $l = 4mm$, for (a). a warm beam, $\gamma = 10^5, \sigma_r = 5\mu m, \sigma_z = 1mm$ and 5×10^{10} particles, the emittance $\epsilon = 5 \times 10^{-10} m - rad$, (b). a cool beam with emittance $\epsilon = 5 \times 10^{-11} m - rad$. The emittances at exit of the plasma lens are $6.9 \times 10^{-10} m - rad$ and 4.8×10^{-10} for (a) and (b) respectively.

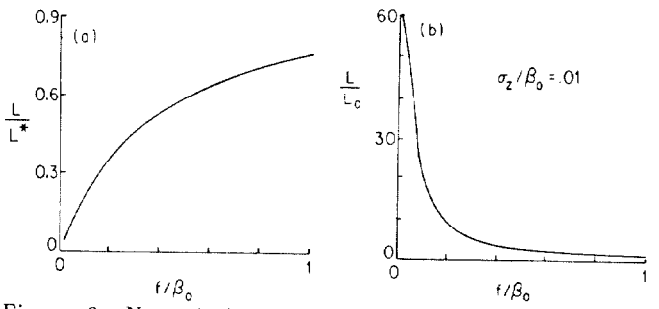

Figure .3: Numerical solution from overdense plasma lenses with logitudinal aberrations included. (a) redution factor $\mathcal{L}/\mathcal{L}^*$ due to logutudinal aberration. (b) luminosity enhancement for $\sigma_z/\beta_0 = 0.01$.

Underdense Plasma Lens $n_b \geq n_0/2$

In the overdense plasma lens described in the previous section, the beam density represented a small perturbation to the plasma density. Thus, the plasma dynamics were well described by linear theory and were similar for electron and positron beams. In the underdense regime, the plasma dynamics become highly nonlinear and differ considerably for electrons and positrons. To describe the plasma lens in this regime we rely on physical models and self-consistent simulations. The underdense plasma lens has several advantages including smaller spherical aberrations and longitudinal aberrations and reduced plasma contribution to background in the detectors of a collider.

In the underdense plasma lens regime the space charge of the e^- beam essentially blows out all of the plasma electrons leaving a uniform column of positive ion charge. The net force on the e^- beam is that of the ions; namely

$$F_r = 2\pi n_0 e^2 r$$

Since the plasma density n_0 is independent of r, the linearity of the focusing force no longer depends on the detailed radial dependence of n_b. Thus we expect spherical aberrations to be very small for e^- beams in an underdense plasma lens.

For positron beams, the plasma dynamics are more complex. The space charge of the beam pulls plasma electron into the beam. However, there are not enough plasma electrons available to completely neutralize the beam. Thus the plasma electron density tends to approach the positron density in the center, and to form a depletion region in the outer part of the beam. The focusing force becomes extremely nonlinear in r in this case. A solution to this problem is then to make the beam radius small ($< \sqrt{n_0/n_b}\, c/\omega_p$) so that the beam only samples the center region where eletron density is large and uniform. To quantitatively describe the phenomena we turn to particle simulations.

Simulations

The simulation code used is ISIS[15]; it is a $2\frac{1}{2}$D fully relativistic self-consistent particle-in-cell code. The $2\frac{1}{2}$D spatial and momentum variables are r, z and p_r, p_z and p_θ.

To examine the underdense plasma lenses for electron and positron beams we inject two 500 Mev e^- and e^+ beam into a system whose dimensions are $140c/\omega_p$ long and $6c/\omega_p$ in radius. The beams' densities are $n_b = 2n_p \exp(-r^2/2\sigma_r^2 - (z \pm ct)^2/2\sigma_z^2)$ for $r \leq 3\sigma_r$ and $| z \pm ct | \leq 3\sigma_z$; where $k_p\sigma_r = 0.3, k_p\sigma_z = 10$. Two plasma lenses are centered at $k_p z = 15$, 125 and are $20c/\omega_p$ long.

Fig. 4(a) is a snapshot of two beams passing through palsma lenses. The e^- beam repels plasma electrons and creates a uniform ion column. The logitudinal aberrations are then absent except near the front and the back edges where the beam density drop below $n_0/2$. The uniform ion column also eliminates spherical aberrations. On the other side the positrons pull plasma electrons into the beam and drag them out of the plasma. Those electrons' density can be as high as the positron beam and the energy can be up to a few Mev. The aberrations are larger than in the electron beam case but smaller or comparable to the overdense plasma lens case.

The positrons near the center experience a uniform focusing strength. The simulation shows the focusing force within $1\sigma_r$ radius is linear in r.

The focusing force of the positron beam is stronger than that of the electron beam. The reason is the focusing strength is proportional to the plasma density for the electron beam case. However, the perturbed plasma electron density in the positron beam case can be as high as the positron density. Thus the focal length differs for electrons and positrons. This is apparent for the simulation of Fig. 4(b). There the best focus of the e^+ beam is $35\,c/\omega_p$ from the lens; for the e^- beam it is $50\,c/\omega_p$.

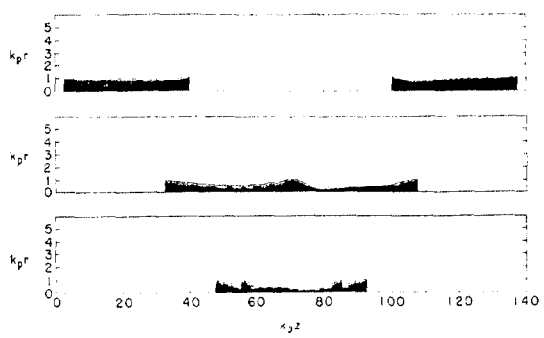

Figure 4: Real space of colliding e^- (right) and e^+ beams showing focusing by plasma lenses and beam-beam disruption.

Fig 4(c) illustrates the collision of two beams. Qualitatively, we see the focusing of one beam by the other. This is well known as the beam-beam disruption[16]. It shows that the luminosity increases by a factor of 40 due to the reduction beam radii by plasma lenses and the beam-beam disruption. To understand separate the contrbution of the luminosity enhancement from plasma lenses and from beam-beam disruption we perform simulations of several cases.

H_D	$\Delta fe^+ = 1.5\sigma_z$	$\Delta f = 0$
$\mathcal{L}_2/\mathcal{L}_0$	40.3	44.4
$\mathcal{L}_2/\mathcal{L}_1$	34.0	37.5
$\mathcal{L}_3/\mathcal{L}_0$	17.2	22.8

Table 1.shows the results for the luminosity enhancement compared to $\mathcal{L}_0$, where $\mathcal{L}_0$ is from integration of Eq. (7). $\mathcal{L}_1$ is the luminosity from simulation result of two beams colliding without plasma lenses (but with disruption). $\mathcal{L}_2$ includes all effects such as the beam-plasma and beam-beam interaction. The beam-beam disruption was taken out from the $\mathcal{L}_3$ case (but plasma lenses remain) .

The two right hand columns of Table 1 show the effect of axial offset of the interaction point relative to the beam focal points. For the first column, the two lenses were symmetric about the I.P. resulting in an offset of the focal point by $15\,c/\omega_p$ for the e^+ beam; for the second column the lens for positrons is moved closer to the I.P. to eliminate the offset. We see that there is a tendency of the disruption to compensate for the reduction in luminosity by only about 10%.

Ackowlegment This work is supported by U.S. DOE contract DE-AS03-83-ER40120, DE-FG03-87ER13752 and NSFPHY 86-11235.

References

1 P.Chen, Particle Accelerator 20, 171 (1987).

2 P.Chen,J.J.Su,T.Katsouleas,S.Wilks abd J.M.Dawson, IEEE Tran. Nucl. Sci. PS-15, 218 (1987).

3 P.J.Channel in Laser Accelerator of Particles (malibu, 1985) AIP Conference Procedings No. 130, C.Joshi and T.Katsouleas, eds. (AIP,NY,1985).

4 R.Fedele, U. de Angelis and T.Katsoutles, Phys. Rev. A 33, 4412 (1986).

5 B.Autin *et al.* IEEE Tran. Plasma Sci., PS-15 226 (1987).

6 T.G.Roberts and W.H.Bernett, Plasma Physics 10, 381 (1968).

7 T.Katsouleas, Phys. Rev. A 33, 2056 (1986).

8 R.D.Ruth, SLAC-PUB-4848, 1989.

9 J.J.Su *et al.*, IEEE Trans. Plasma Sci. PS-15, 192 (1987).

10 J.Rosenzweig and P.Chen, SLAC-PUB-4571, March 1988.

11 J.J.Su, T.Katsouleas, J.M.Dawson and R.Fedele, UCLA-PPG-1177, submitted to Phy . Rev. A.

12 Erickson, SLAC-PUB-4479,1987.

13 G.Gisler *et al.*, Proc. 11th Int'l Conf. Num. Sim. of Plasma, (Quebec, Canada, 1985).

14 R.Hollebeek, Nucl. Ins. Meth. 184 1981.